Redox Biology 26 (2019) 101264

Contents lists available at ScienceDirect

Redox Biology

journal homepage: www.elsevier.com/locate/redox

The effect of exposure time and concentration of airborne $PM_{2.5}$ on lung injury in mice: A transcriptome analysis

Hongyun Wang[1], Xiyue Shen[1], Jingli Liu, Chunyan Wu, Junling Gao, Zezhong Zhang, Fang Zhang, Wenjun Ding[**], Zhongbing Lu[*]

College of Life Science, University of Chinese Academy of Sciences, Beijing, 100049, China

ARTICLE INFO

Keywords:
$PM_{2.5}$
Lung injury
RNA-Sequencing
Inflammation
Oxidative stress

ABSTRACT

The association between airborne fine particulate matter ($PM_{2.5}$) concentration and the risk of respiratory diseases has been well documented by epidemiological studies. However, the mechanism underlying the harmful effect of $PM_{2.5}$ has not been fully understood. In this study, we exposed the C57BL/6J mice to airborne $PM_{2.5}$ for 3 months (mean daily concentration ~50 or ~110 μg/m^3, defined as $PM_{2.5}$–3L or $PM_{2.5}$–3H) or 6 months (mean daily concentration ~50 μg/m^3, defined as $PM_{2.5}$–6L) through a whole-body exposure system. Histological and biochemical analysis revealed that $PM_{2.5}$–3H exposure caused more severe lung injury than did $PM_{2.5}$–3L, and the difference was greater than that of $PM_{2.5}$–6L vs $PM_{2.5}$–3L exposure. With RNA-sequencing technique, we found that the lungs exposed with different concentration of $PM_{2.5}$ have distinct transcriptional profiles. $PM_{2.5}$–3H exposure caused more differentially expressed genes (DEGs) in lungs than did $PM_{2.5}$–3L or $PM_{2.5}$–6L. The DEGs induced by $PM_{2.5}$–3L or $PM_{2.5}$–6L exposure were mainly enriched in immune pathways, including Hematopoietic cell lineage and Cytokine-cytokine receptor interaction, while the DEGs induced by $PM_{2.5}$–3H exposure were mainly enriched in cardiovascular disease pathways, including Hypertrophic cardiomyopathy and Dilated cardiomyopathy. In addition, we found that upregulation of *Cd5l* and reduction of *Hspa1* and *peroxiredoxin-4* was associated with $PM_{2.5}$-induced pulmonary inflammation and oxidative stress. These results may provide new insight into the cytotoxicity mechanism of $PM_{2.5}$ and help to development of new strategies to attenuate air pollution associated respiratory disease.

1. Introduction

Currently, ambient air pollution has become a large threat to public health. Fine particulate matter ($PM_{2.5}$, aerodynamic diameter ≤ 2.5 μm) is one of the most important components of outdoor air pollution. High concentration of $PM_{2.5}$ increases the risk of respiratory diseases, including asthma [1], bronchitis [2], chronic obstructive pulmonary disease (COPD) [3] and lung cancer [4,5]. Using an analysis of daily time-series for the 20 largest US cities, the PM-mortality dose-response curves and threshold levels were firstly described in 2000 [6]. Then, multiple epidemiological studies have validated that there is a concentration-response relationship between airborne $PM_{2.5}$ and its harmful effects on respiratory system [5,7–9]. In mice models, a recent study found that the severity of lung injury caused by ambient PM exposure is associated with cumulative dose [10]. Acute exposure to low doses of fine PM by intranasal instillation also induced lung inflammation and oxidative stress in a dose-dependent manner [11]. It has been suggested that $PM_{2.5}$-induced inflammatory response was associated with Toll-like receptors (TLR2/TLR4) and $PM_{2.5}$ can drive a Th2-biased immune response in mice [12]. Notably, during inflammation induced by $PM_{2.5}$, enhanced production of reactive oxygen species (ROS) could result in DNA damage, lipid peroxidation and cell death [13–15]. However, the comprehensive mechanisms by which $PM_{2.5}$ causes lung injury have not been full elucidated.

RNA-sequencing (RNA-seq) is a precise and sensitive tool for measuring global gene expression profiles expression. Recently, this technique has been used to investigate the mechanism of $PM_{2.5}$-induce cytotoxicity in cell models, including 16HBE [16], BEAS-2B [17], A549 [18] and human non-small-cell lung cancer (H1299) cells [19]. To better understand the harmful effects of $PM_{2.5}$ on respiratory system, we exposed mice to either airborne $PM_{2.5}$ or filtered air (FA) for 3–6 months through a whole-body exposure system and then obtained global gene expression profiles in lungs of FA or $PM_{2.5}$ exposed mice using RNA-seq.

[*] Corresponding author.College of Life Science, University of Chinese Academy of Sciences, 19A Yuquanlu, Beijing, 100049, China.
[**] Corresponding author., College of Life Science, University of Chinese Academy of Sciences, 19A Yuquanlu, Beijing, 100049, China.
E-mail addresses: dingwj@ucas.ac.cn (W. Ding), luzhongbing@ucas.ac.cn (Z. Lu).
[1] These two authors contributed equally to this work.

https://doi.org/10.1016/j.redox.2019.101264
Received 30 April 2019; Received in revised form 18 June 2019; Accepted 30 June 2019
Available online 02 July 2019

Abbreviations

3′-NT	3-nitrotyrosine
4-HNE	4-hydroxynonenal
BALF	bronchoalveolar lavage fluid
Cd5l	CD5 antigen-like
COPD	chronic obstructive pulmonary disease
DCM	dilated cardiomyopathy
DEGs	differentially expressed genes
FA	filtered air
Gpx	glutathione peroxidase
GSH	reduced glutathione
GSSG	oxidized glutathione
H&E	hematoxylin and eosin
HCM	hypertrophic cardiomyopathy
Hspa1	heat shock 70 kDa protein 1
IL	interleukin
ILr	interleukin receptor
KEGG	kyoto encyclopedia of genes and genomes
Ndufs	NADH dehydrogenase iron-sulfur protein
PM	particulate matter
Prdx4	peroxiredoxin-4
qPCR	quantitative real-time polymerase chain reaction
RNA-seq	RNA-sequencing
ROS	reactive oxygen species
Sod	superoxide dismutase
TLR	Toll-like receptors
TNFα	Tumor Necrosis Factor
TNFrsf	TNF receptor superfamily member 14
Trxn	thioredoxin
Trxr2	thioredoxin reductase

2. Materials methods

2.1. Reagents and antibodies

BCA protein assay kit and reduced/oxidized glutathione (GSH and GSSG) kit were purchased from the Beyotime Institute of Biotechnology (#P0012, #S0053, Shanghai, China). Elisa kits for mouse tumor necrosis factor alpha (TNFα), 3′-nitrotyrosine (3′-NT) and 4-hydroxynonenal (4-HNE) were purchased from Sino Biological Inc (#SEK50349, Beijing, China), Abcam PLC (#ab116691, Cambridge, UK) and Donggeboye Biological Technology Co. LTD (#DG30947 M, Beijing, China), respectively. The Masson's trichrome stain kit and superoxide dismutase 3 (SOD3) antibody were obtained from Solarbio Science &Technology Co. LTD (#G1340, #K006598P, Beijing, China). Primary antibodies against β-tubulin, SOD1, SOD2, peroxiredoxin 3 (PRDX3), PRDX4, PRDX5 and thioredoxin reductase 2(TRXR2) were purchased from Signalway Antibody LLC (#38075, #32058, #32265, #38567, #43303, #38828, #32885, College Park, MD, USA). Anti-galectin 3 and neutrophil antibodies were purchased from Bioss Biotechnology Co. LTD (#bs-20700R, #bs-6982R, Beijing, China).

2.2. Animal experiments

As described previously [20], male C57BL/6J mice (20–22g, obtained from HFK Bioscience Co., Beijing, China) were exposed to either ambient $PM_{2.5}$ or FA in a “real-world” exposure system for 12 h/day, 7 days/week, for 3–6 months (October–December 2015 or July–December 2017). The exposure system contains two chambers and ambient air was inhaled into the chambers by air pump. In the inlet valve of FA chamber, a high efficiency particulate air filter (Shanghai Liancheng Purification Equipment CO., LTD, Shanghai) was installed to remove all the microparticles. In the $PM_{2.5}$ exposure chamber, PM with an aerodynamic diameter greater than 2.5 μM was removed by a swirler. The exposure system locates at Zhongguancun campus of the University of Chinese of Academy of Sciences (N39°57′39.83″E116°20′10.97″), which is ~50 m away from a traffic main artery (Sihuan Road). During the whole exposure stage, the mice were fed commercial mouse chow and distilled water *ad libitum*, and were housed under a controlled temperature (22 ± 2 °C) and relative humidity (40–60%) with a 12 h light/dark cycle. Animal studies were performed in accordance with the principles of laboratory animal care (NIH publication no. 85–23, revised 1985) and with approval by the University Of Chinese Academy of Sciences Animal Care and Use Committee.

2.3. Bronchoalveolar lavage

The mice were anesthetized by pentobarbital sodium after exposure. Then, the whole lungs were lavaged 3 times with 1 ml phosphate buffer solution (PBS, pH = 7.4). The bronchoalveolar lavage fluid (BALF) was collected and centrifuged at 1000 rpm for 5–10 min. Total cell number and the protein content of the BALF were measured respectively.

2.4. Histologic assessment

Mouse lungs were harvested quickly, and then washed with ice-cold PBS for three times. After fixation with 4% paraformaldehyde for 48 h, the lungs were embedded in paraffin. Tissue sections (5 μm) were stained with hematoxylin and eosin (H&E) or Masson trichrome staining kits. To identify macrophages and neutrophils, tissue sections were stained with anti-galectin 3 and anti-neutrophil monoclonal antibodies, respectively.

2.5. RNA isolate and RNA-sequencing

Total RNA was extracted from the lungs of FA- or $PM_{2.5}$-exposed mice using TRIzol reagent (Invitrogen, Carlsbad, CA, USA). RNA quality was measured by Agilent 2100 bioanalyzer (Thermo Fisher Scientific, MA, USA) and samples with an RNA integrity number over than 8 were used for subsequent experiments. The total RNA was further purified by digesting the double-stranded and single-stranded DNA with DNase I and remove of rRNA using Ribo-Zero method (human, mouse, plants) (Illumina, USA). The library construction and RNA sequencing were performed on a BGISEQ500 platform (BGI-Shenzhen, China).

2.6. Read mapping and differentially expressed gene analysis

The raw data were firstly counted and cleaned using SOAPnuke (BGI-Shenzhen, China) and trimmomatic [21] software to remove ligation sequence, low quality sequence and repeats. The sequencing data for clean reads generated by this study have been deposited in the NCBI Sequence Read Archive (SRA) database (accession number: PRJNA540011). Then the clean reads were mapped to the reference genome (Mus_musculus, GCF_000001635.25_GRCm38.p5) using HISAT (Hierarchical Indexing for Spliced Alignment of Transcripts) [22] or Bowtie 2 [23] software. The matched reads were calculated and then normalized to RPKM value (reads per kilo base per million mapped reads) using RESM software [24] to obtain the gene expression level. The differential expression of genes (DEGs) between two groups was screened by DEGseq [25] with the thresholds of fold change ≥ 2 and adjusted P value ≤ 0.001.

To further understand the biological functions of genes, the identified DEGs in each pair were mapped to terms in the Kyoto Encyclopedia of Genes and Genomes (KEGG) database (http://www.genome.jp/kegg/pathway.html). In addition, we performed enrichment analysis using the phyper function of R software. The p-value was adjusted for

false discovery rate (FDR) to get q-value, and q-value ≤ 0.05 was considered as significant enrichment.

2.7. Quantitative real-time PCR analysis and western blot

The cDNA was synthesized using a PrimeScript RT Reagent Kit (#RR036B, TaKaRa, Otsu, Japan) and mRNA expression were measured by quantitative real-time polymerase chain reaction (qPCR) with the SYBR® Premix Ex Taq™ II Kit (#RR820A). The results were normalized to 18S ribosomal RNA. Primers used in this study are listed in Table S1.

Proteins were extracted from mouse lung using lysis buffer (150 mM NaCl, 100 μg/ml phenylmethylsulfonyl fluoride, 50 mM Tris-Cl and 1% Triton X-100) with protease and phosphatase inhibitor cocktail (#04693124001, #4906837001, Roche, Basel, Switzerland) on 4 °C for 20–30 min. After centrifugation at 12,000 g and 4 °C for 20 min, the supernatant was used for western blot analysis as reported previously [20].

2.8. Statistical analysis

All data were analyzed by StatView (SAS Institute Inc.) and expressed as mean ± SEM. One-way analysis of variance (ANOVA) with Tukey's correction was used to make multiple comparisons among the groups. $p < 0.05$ was defined statistical significance.

3. Results

3.1. Effect of exposure time and concentration on $PM_{2.5}$-induced lung inflammation & fibrosis

The average monthly concentration of $PM_{2.5}$ during the exposed period was calculated based on the daily data from http://datacenter.mep.gov.cn/. The experiment groups were defined as $PM_{2.5}$–3L group (exposed from July to September in 2017, average concentration ~50 μg/m^3), $PM_{2.5}$–6L group (exposed from July to December in 2017, average concentration ~50 μg/m^3) and $PM_{2.5}$–3H group (exposed from October to December in 2015, average concentration ~115 μg/m^3) (Fig. 1A). As to FA-exposed mice, 3 months or 6 months exposure had no obvious difference in lung morphology, BALF cell flux and serum tumor necrosis factor (TNFα) levels. Therefore, the mice exposed to FA from July to September in 2017 were used as the control group.

To determine whether $PM_{2.5}$ concentration or exposure time affects pulmonary alveoli injury, the cell flux and protein content in BALF were measured. As shown in Fig. 1B–C, $PM_{2.5}$ exposure significantly increased the cell number and protein concentration of BALF. In addition, BALF from $PM_{2.5}$–3H mice had significantly more cell number and higher protein concentration than that of $PM_{2.5}$–3L mice, while the differences in cell number and protein concentration of BALF between $PM_{2.5}$–3L and $PM_{2.5}$–6L groups were not significant (Fig. 1B–C). Although serum TNFα levels were elevated in $PM_{2.5}$-exposed mice, there was no obvious difference among $PM_{2.5}$–3L, $PM_{2.5}$–6L and $PM_{2.5}$–3H groups (Fig. 1D).

As revealed by H&E and Masson staining, $PM_{2.5}$ exposure resulted in obvious lung injury & fibrosis, as indicated by the collapse of alveoli, airway epithelial thickening and collagen deposition. Histopathological analysis of lung sections further demonstrated that lungs from $PM_{2.5}$–6L or $PM_{2.5}$–3H group developed significantly more severe injury and fibrosis than lungs from FA or $PM_{2.5}$–3L group. Immunohistochemical staining by antibodies specific for macrophage marker (galectin-3) and neutrophil also revealed that lungs from $PM_{2.5}$–3H group exhibited more infiltration of macrophages and neutrophils than lungs from FA or $PM_{2.5}$–3L group (Fig. 2). Together, these results indicated that the degree of lung injury was associated with the $PM_{2.5}$ concentration and exposure time.

3.2. $PM_{2.5}$ exposure changed gene expression profile in mice lungs

To investigate the molecular mechanism by which $PM_{2.5}$ exposure causes lung injury in mice, RNA-sequencing was performed to analysis the whole-genome expression profiling changes in $PM_{2.5}$-exposed lungs. Boxplot showed the general distribution of genes expression of mice lungs from FA, $PM_{2.5}$–3L, $PM_{2.5}$–6L and $PM_{2.5}$–3H groups (Fig. S1). A total of 455 DEGs (311 up-regulated and 144 down-regulated) were identified in comparison of FA and $PM_{2.5}$–3L exposed lungs, and the fold change of these DEGs were visualized by Volcano plot (Fig. 3A–B). The top 10 up- and down-regulated genes were listed in Table S2. Among these genes, *Prok2*, *Ccl19, Ucp1*, *Gm13277*, *Pet117*, *Tat*, *Nkx6-2* and *Bnc1* are involved in inflammation and oxidative stress related biological process. We also identified 545 DEGs (376 up-regulated and 169 down-regulated) from FA vs $PM_{2.5}$–6L group and 1133 DEGs (887 up-regulated and 246 down-regulated) from FA vs $PM_{2.5}$–3H group (Fig. 3A). The fold change of these DEGs from FA vs $PM_{2.5}$–6L and FA vs

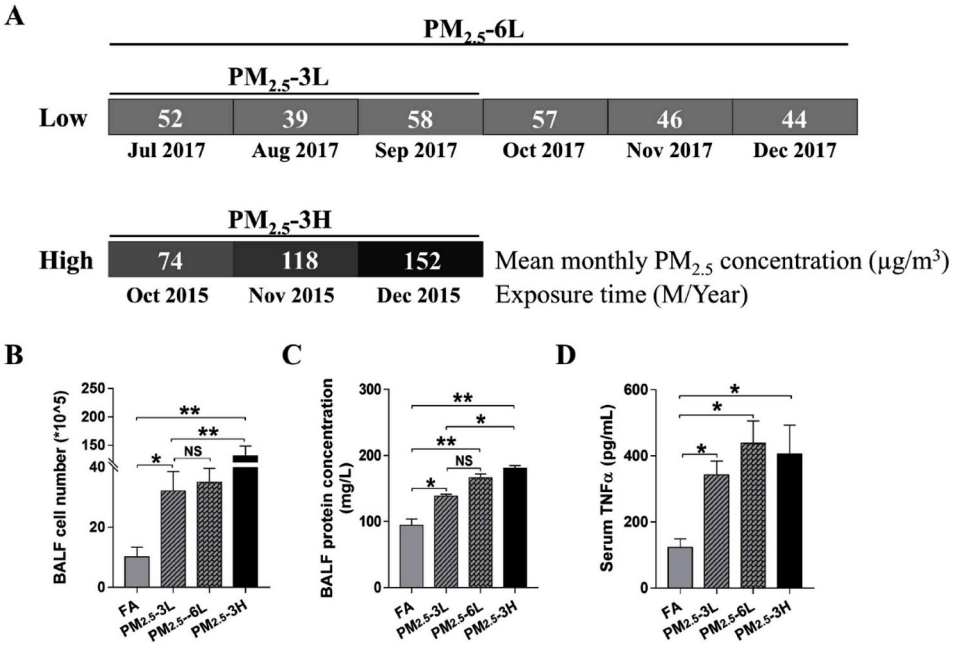

Fig. 1. Effect of exposure time and concentration on $PM_{2.5}$-induced systematic inflammation and lung injury. $PM_{2.5}$ concentration of Wanliu monitoring station was recorded during the exposure period. Mean monthly $PM_{2.5}$ concentration of July, August, September, October, November and December in 2017, as well as October, November and December in 2015 were shown (A). After exposure to filtered air (FA), low concentration of $PM_{2.5}$ for 3–6 months ($PM_{2.5}$–3L, $PM_{2.5}$–6L) or high concentration of $PM_{2.5}$ ($PM_{2.5}$–3H) for 3 months, total cell number (B) and protein content (C) in bronchoalveolar lavage fluid (BALF), and serum TNFα level was measured (D). Data are presented as the means ± SEM. N = 3–4. *p < 0.05; **p < 0.01; NS, not significant.

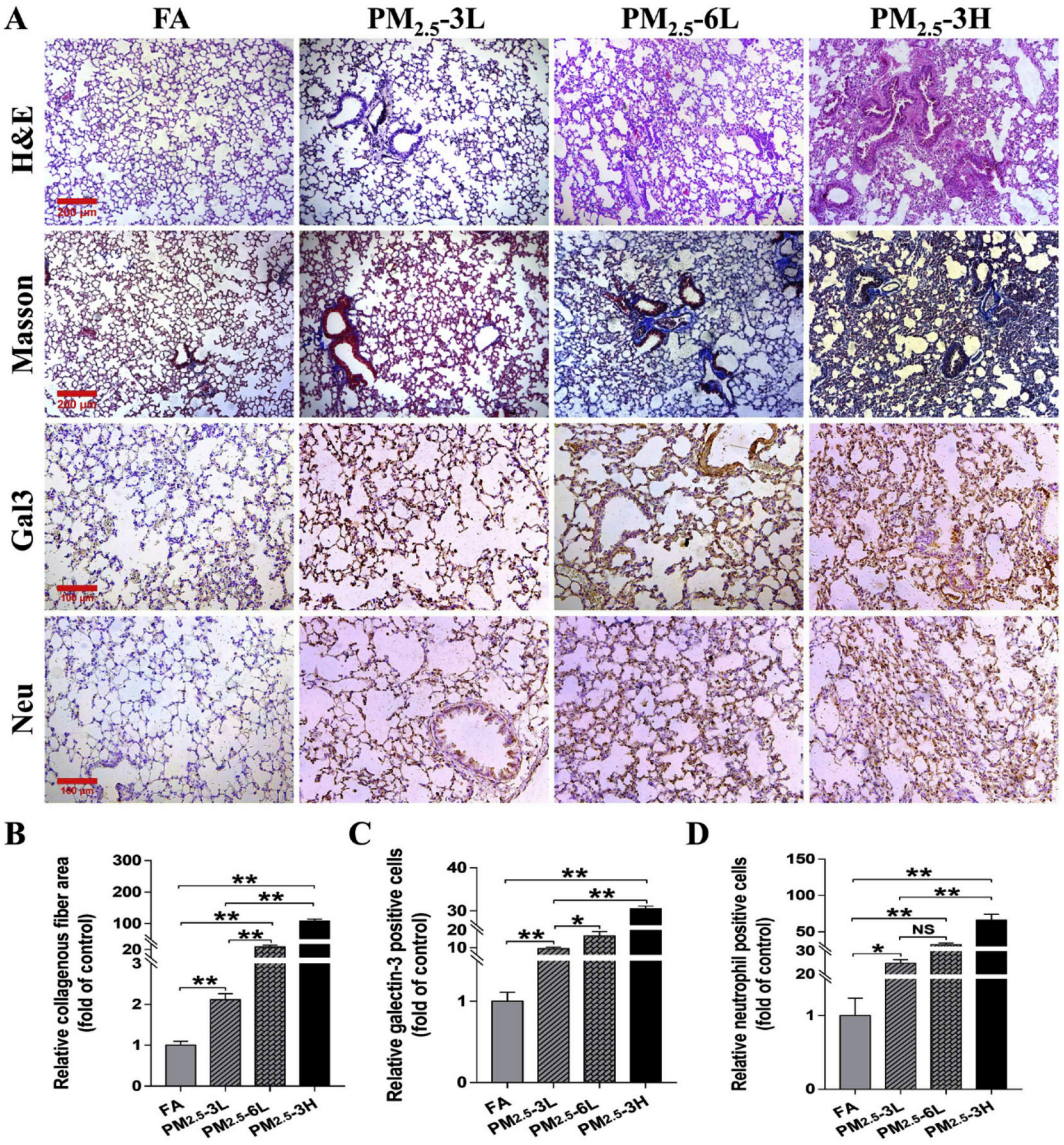

Fig. 2. Effect of exposure time and concentration on $PM_{2.5}$-induced pulmonary fibrosis and inflammation. (A) Representative lung sections from FA, $PM_{2.5}$–3L, $PM_{2.5}$–6L and $PM_{2.5}$–3H exposed mice were stained with hematoxylin and eosin (H&E, Scale bar = 200 μm), Masson trichrome (Scale bar = 200 μm), and antibodies specific for macrophages (galetin-3, Gal-3) and neutrophils (brown staining). Scale bar = 100 μm. The relative collagenous fiber area (B), Gal-3 (C) or neutrophil (D) positive cell number were quantified by Image J software. Data were shown as means ± SEM. N = 4, *p < 0.05; ** indicates p < 0.01; NS, not significant. (For interpretation of the references to color in this figure legend, the reader is referred to the Web version of this article.)

$PM_{2.5}$–3H groups were presented in Supplemental Figs. 2–3 and the top 10 up- and down-regulated genes of each pair were listed in Supplemental Tables 3–4. Among these genes, *Gm1987*, *Ccl19*, *LOC100043921*, *DXBay18*, *Pet117*, *2310045n01rik-mef2b*, *Mpo*, *Hspa1b*, *Gm13305* (from FA vs $PM_{2.5}$–6L group), *Sim2*, *Ifag*, *Spag11b*, *Lep*, *Lhx1* (from FA vs $PM_{2.5}$–3H group) and *2310045n01rik-mef2b* (from both) may participate in regulation of oxidative stress and inflammation related pathway. Interestingly, the top 8 up-regulated genes, including *Mybpc1*, *Myh8*, *Myh4*, *Tnnc2*, *Myot*, *Myh1*, *Acta1* and *Jsrp1*, are involved in of muscle contraction regulation.

Next, we created a Venn diagram to visual depiction of the similarities and differences between the DEGs in each pair. As shown in Fig. 3C, there were 188 overlapped DEGs between FA vs $PM_{2.5}$–3L and FA vs $PM_{2.5}$–6L, 158 overlapped DEGs between FA vs $PM_{2.5}$–3L and FA vs $PM_{2.5}$–3H, and only 55 overlapped DEGs among the three groups. According to the KEGG annotation and official classification, we mapped the DEGs of each pair to KEGG pathways, and the results were presented in Fig. 3D and Figs. S2–S3. Among these perturbed pathways, signal transduction and immune system have the highest numbers of DEGs. We then performed KEGG pathway enrichment analysis and found that many DEGs from FA vs $PM_{2.5}$–3L or FA vs $PM_{2.5}$–6L were significantly enriched in immune pathways, including hematopoietic cell lineage, cytokine-cytokine receptor interaction and B cell receptor signaling pathway (Tables 1–2). We also found that the DEGs of FA vs $PM_{2.5}$–3H group were significantly enriched in inflammation and immune pathways, including Malaria, and Amoebiasis. However, the top 3 most significantly enriched KEGG pathways (Hypertrophic cardiomyopathy (HCM), Dilated cardiomyopathy (DCM) and Cardiac muscle contraction) are associated with cardiovascular disease (Table 3). The DEGs were also significantly enriched in some metabolic pathways, including PPAR signaling pathway, Insulin secretion, Pancreatic secretion, Glycolysis/Gluconeogenesis and Adipocytokine signaling pathway.

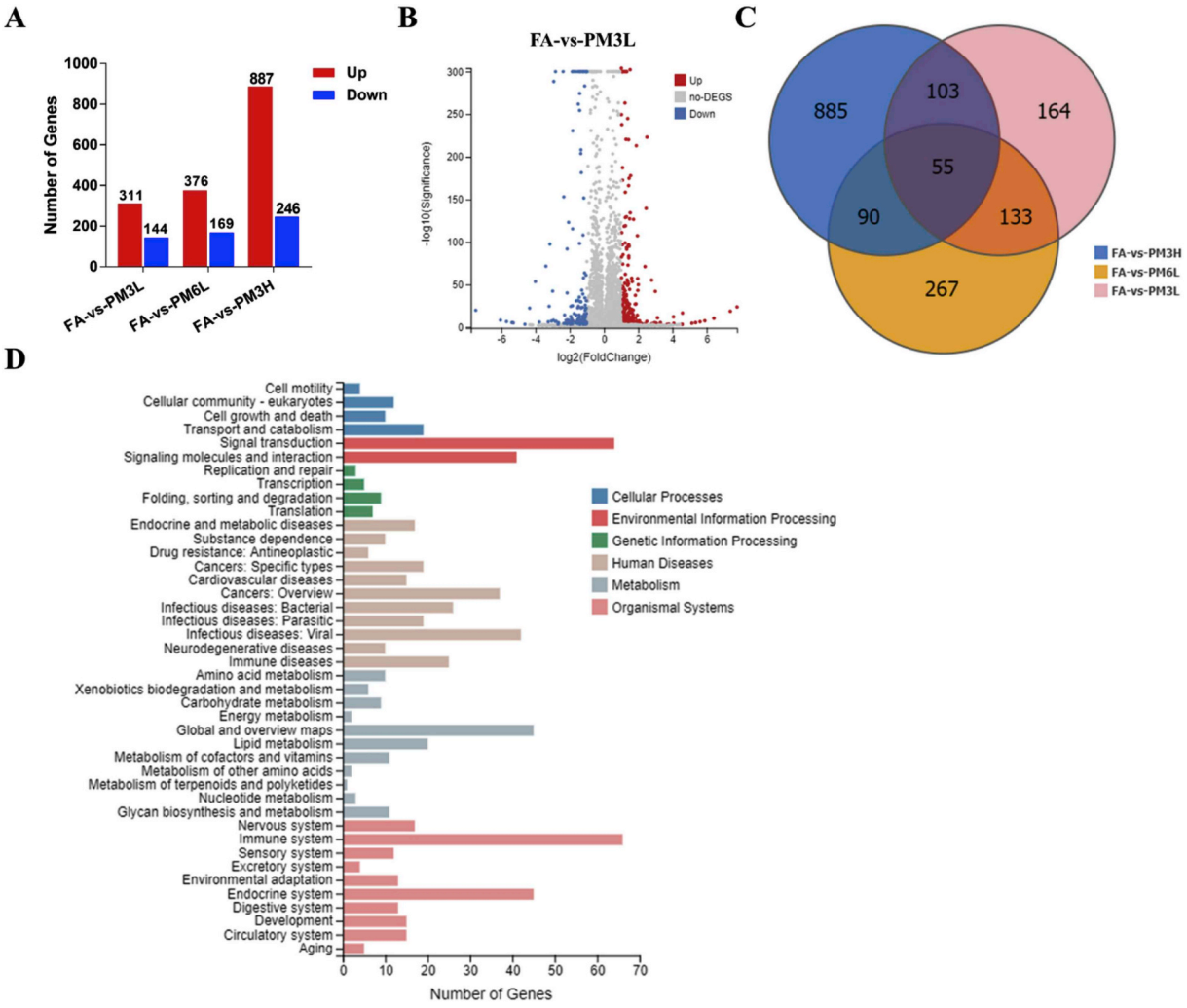

Fig. 3. Analysis of differentially expressed genes between FA and $PM_{2.5}$-exposed mice lungs. (A) Summery of the number of up- and down-regulated genes in the $PM_{2.5}$-3L-, $PM_{2.5}$-6L-, and $PM_{2.5}$-3H-exposed lungs versus FA-exposed lung. Fold change ≥ 2 and adjusted p value ≤ 0.001 were used as the threshold to judge the significance of gene expression difference. (B) The fold change of differentially expressed genes (DEGs) of FA vs $PM_{2.5}$–3L were visualized by Volcano plot. (C) The number of different and overlapped DEGs from FA vs $PM_{2.5}$–3L, FA vs $PM_{2.5}$–6L and FA vs $PM_{2.5}$–3H group were illustrated in Venn diagram. (D) KEGG classification of DEGs from FA vs $PM_{2.5}$–3L group. The functions of genes identified cover six main categories: cellular processes, environmental information processing, genetic information processing, human disease, metabolism and organismal system.

3.3. Effect of exposure time and concentration on gene expression profile in $PM_{2.5}$-exposed lungs

To investigate the effect of exposure time and concentration on gene expression profile in $PM_{2.5}$-exposed lungs, we also identified 235 DEGs (113 up-regulated and 122 down-regulated) from $PM_{2.5}$–3L vs $PM_{2.5}$–6L group and 1201 DEGs (761 up-regulated and 440 down-regulated) from $PM_{2.5}$–3L vs $PM_{2.5}$–3H group, respectively (Fig. 4A). The fold change of these DEGs from $PM_{2.5}$–3L vs $PM_{2.5}$–6L and $PM_{2.5}$–3L vs $PM_{2.5}$–3H group were visualized by Volcano plot (Figs. S4–S5). Among all the DEGs in the volcano plots, top 10 up- and down-regulated genes of $PM_{2.5}$–3L vs $PM_{2.5}$–6L and $PM_{2.5}$–3L vs $PM_{2.5}$–3H were listed in Tables

Table 1
Significantly enriched KEGG pathway of DEGs in FA vs $PM_{2.5}$–3L group.

Pathway ID	Pathway Name	Gene Number	Rich Ratio[a]	Q value
ko04640	Hematopoietic cell lineage	14	0.11864407	4.91E-05
ko04060	Cytokine-cytokine receptor interaction	20	0.05464481	0.01323701
ko04662	B cell receptor signaling pathway	9	0.09	0.01786184
ko05150	*Staphylococcus aureus* infection	8	0.10126582	0.01786184
ko04612	Antigen processing and presentation	11	0.07142857	0.02054528
ko04672	Intestinal immune network for IgA production	6	0.12244898	0.02054528
ko04710	Circadian rhythm	5	0.15151515	0.02054528
ko05323	Rheumatoid arthritis	9	0.08181818	0.02054528
ko04711	Circadian rhythm - fly	3	0.33333333	0.02206418
ko04514	Cell adhesion molecules (CAMs)	14	0.05555556	0.02559195

[a] Rich ratio is defined as amount of differentially expressed genes enriched in the pathway/amount of all genes in background gene set.

Table 2
Significantly enriched KEGG pathway of DEGs in FA vs $PM_{2.5}$–6L group.

Pathway ID	Pathway Name	Gene Number	Rich Ratio	Q value
ko04640	Hematopoietic cell lineage	16	0.13559322	1.05E-05
ko04060	Cytokine-cytokine receptor interaction	27	0.073770492	7.06E-05
ko05310	Asthma	9	0.2	0.000127211
ko04662	B cell receptor signaling pathway	11	0.11	0.00239461
ko04711	Circadian rhythm - fly	4	0.444444444	0.00239461
ko04062	Chemokine signaling pathway	18	0.071428571	0.003007857
ko03320	PPAR signaling pathway	11	0.094017094	0.006579429
ko05134	Legionellosis	8	0.103896104	0.02277741
ko04672	Intestinal immune network for IgA production	6	0.12244898	0.03628709
ko04710	Circadian rhythm	5	0.151515152	0.03628709
ko04612	Antigen processing and presentation	11	0.071428571	0.04275478

S5 and S6, respectively. Although Venn diagram showed that there were 111 overlapped DEGs (Fig. 4B), the top 10 up-regulated of genes in $PM_{2.5}$ 3L-vs $PM_{2.5}$–3H are totally different from those of $PM_{2.5}$–3L vs $PM_{2.5}$–6L. There are three overlapped top down-regulated genes, including *Rps27rt*, *GM40369* and *Pcdha9*. The functions of *Rps27rt* and *GM40369* remain unclear, while *Pcdha9* mutation is associated with Hirschsprung's disease [26].

We also mapped the DEGs of each pair to KEGG pathways, and most of DEGs belonged to signal transduction and immune pathways (Figs. S4–S5). KEGG pathway enrichment analysis demonstrated that the DEGs of $PM_{2.5}$–3L vs $PM_{2.5}$–6L were only significantly enriched in Cytokine-cytokine receptor interaction pathway, while the DEGs of $PM_{2.5}$–3L vs $PM_{2.5}$–3H were significantly enriched in inflammation and immune pathways (Hematopoietic cell lineage, Amoebiasis, *Staphylococcus aureus* infection, Cytokine-cytokine receptor interaction, and etc.) and cardiovascular disease pathways (Hypertrophic cardiomyopathy, Dilated cardiomyopathy and Cardiac muscle contraction) (Fig. 4C, Table S6).

3.4. Down-regulation of Hspa1 and up-regulation of Cd5l were associated with $PM_{2.5}$-induced pulmonary inflamation

To explore the mechanism for the activated immune pathway in $PM_{2.5}$-exposed lungs, the expression profile of some inflammatory response related genes, including *chemokine (C–C motif) ligand* (CCL), *interleukin* (IL), *interleukin receptor* (ILr), *tumor necrosis factor receptor superfamily* (*Tnfrsf*), *heat shock* 70 kDa *protein* (Hspa) and *cluster of differentiation* (CD), were shown in the heat map (Fig. 5A). We also performed real-time qPCR to validate the changes of some genes, including heat shock protein family A member 1A (*Hspa1a)* and *Hspa1b*, *Fis1* (mitochondrial fission), *CD14* (endotoxin receptor), *Tnfrsf4* and *CD5 antigen-like (Cd5l)*. We found that *Hspa1a*, *Hspa1b, Fis1* and *CD14* were significantly down-regulated in $PM_{2.5}$-exposed lungs (Fig. 5B–E). In addition, the mRNA levels of *Hspa1a* and *Hsap1b* were further markedly decreased in $PM_{2.5}$–6L and $PM_{2.5}$–3H lungs (Fig. 5B–C). We also found that $PM_{2.5}$ exposure significantly increased the mRNA levels of *Cd5l* via a concentration-dependent manner (Fig. 5F). Previous reports demonstrated that *Hspa1* protects against TNFα-induced lethal inflammatory shock and cell death [27,28], while overexpression of *Cd5l* in alveolar type II epithelial cells induces spontaneous lung adenocarcinoma [29]. Thus, it is likely that the reduction of *Hspa1a and Hsap1b* expression, as well as upregulation of *Cd5l*, might be important factors for the lung injury and pulmonary inflammation induced by $PM_{2.5}$–3H exposure. Although heat map indicated that the expression of *Tnfrsf4* was increased in lungs of $PM_{2.5}$-exposed mice, qPCR results demonstrated that the up-regulation of *Tnfrsf4* was not statistic significant (Fig. 5G).

3.5. Down-regulation of Prdx4 was associated with $PM_{2.5}$-induced pulmonary oxidative stress

$PM_{2.5}$–3L exposure resulted in slightly decrease in the GSH/GSSG ratio and moderately increase of 3′-NT and 4-HNE levels, and the changes in GSH/GSSG ratio and 4-HNE levels were not significant. However, compared with FA-exposed lungs, $PM_{2.5}$-6L- and $PM_{2.5}$-3H-exposed lungs exhibited significantly lower GSH/GSSG ratio and higher 3′-NT and 4-HNE levels (Fig. 6A–C). We also compared the oxidative stress degree in lung of $PM_{2.5}$-exposed mice. There was no significantly difference between $PM_{2.5}$–6L and $PM_{2.5}$–3L groups. However, $PM_{2.5}$–3H lungs exhibited significantly lower GSH/GSSG ratio and higher levels of 3′-NT and 4-HNE than those of $PM_{2.5}$–3L lungs (Fig. 6A–C), indicating that $PM_{2.5}$ exposure causes pulmonary oxidative stress via a concentration-dependent manner.

Table 3
Significantly enriched KEGG pathway of DEGs in FA-vs-$PM_{2.5}$–3H group.

Pathway ID	Pathway Name	Gene Number	Rich Ratio	Q value
ko05410	Hypertrophic cardiomyopathy (HCM)	21	0.165354331	0.000145656
ko05414	Dilated cardiomyopathy (DCM)	21	0.1640625	0.000145656
ko04260	Cardiac muscle contraction	17	0.184782609	0.000195424
ko03320	PPAR signaling pathway	18	0.153846154	0.001089685
ko05144	Malaria	12	0.176470588	0.006066107
ko04261	Adrenergic signaling in cardiomyocytes	22	0.114583333	0.008971435
ko04510	Focal adhesion	32	0.09495549	0.01093564
ko04964	Proximal tubule bicarbonate reclamation	7	0.25	0.011916956
ko04974	Protein digestion and absorption	18	0.119205298	0.014059568
ko05146	Amoebiasis	19	0.113095238	0.017217277
ko04512	ECM-receptor interaction	17	0.114864865	0.025215623
ko04010	MAPK signaling pathway	33	0.084398977	0.033563343
ko04911	Insulin secretion	13	0.12745098	0.033563343
ko04972	Pancreatic secretion	15	0.11627907	0.033563343
ko05412	Arrhythmogenic right ventricular cardiomyopathy (ARVC)	13	0.125	0.033563343
ko00010	Glycolysis/Gluconeogenesis	12	0.129032258	0.035681392
ko04920	Adipocytokine signaling pathway	12	0.127659574	0.03683053

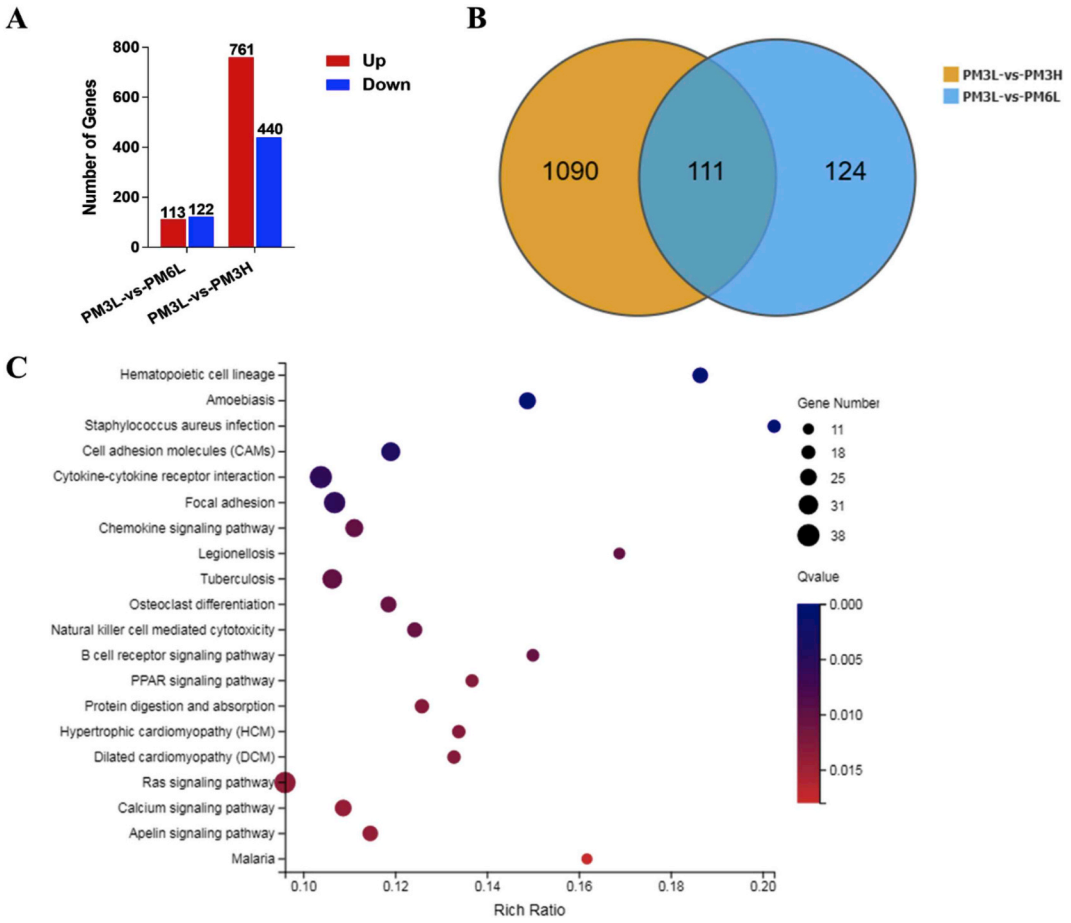

Fig. 4. Effect of exposure time and concentration on gene expression profile in $PM_{2.5}$-exposed lungs. (A) Summery of the number of up- and down-regulated genes in the $PM_{2.5}$-6L-, and $PM_{2.5}$-3H-exposed lungs vs $PM_{2.5}$–3L -exposed lung. Fold change ≥ 2 and adjusted p value ≤ 0.001 were used as the threshold to judge the significance of gene expression difference. (B) Venn diagram shows the number of different and overlapped DEGs from $PM_{2.5}$–3L vs $PM_{2.5}$–6L and $PM_{2.5}$–3L vs $PM_{2.5}$–3H group. (C) Advanced bubble chart shows the top 20 significantly enriched KEGG pathways of DEGs in $PM_{2.5}$–3L vs $PM_{2.5}$–3H group. *Y*-axis label represents pathway, and *X*-axis label represents rich ratio. Size and color of the bubble represent amount of DEGs enriched in pathway and enrichment significance, respectively. (For interpretation of the references to color in this figure legend, the reader is referred to the Web version of this article.)

To investigate the underlying mechanism for the increased oxidative stress in $PM_{2.5}$–3H lungs, some oxidative-related genes (*Gpx, Prdx, Sod, Txn, Txnrd, and Ndufs*) expression profile were demonstrated as the heat map (Fig. 6D). From the heat map, we found that only *Prdx4* and *Sod3* were down-regulated, while other anti-oxidative genes were up regulated in $PM_{2.5}$–3H lungs. To confirm the changes in these anti-oxidant genes, we also examined the protein expression of PRDX (as PRDX3, PRDX4, and PRDX5), SOD (SOD1, SOD2, and SOD3) and TRXR2 in lung lysates by western blot. As shown in Fig. 6E, $PM_{2.5}$ exposure significantly decreased SOD2, SOD3 and PRDX4 expression in all groups, whereas had no obvious effect on PRDX5 and TRXR2 expression. PRDX3 expression was slightly increased in $PM_{2.5}$–3L lungs, and was significantly elevated in $PM_{2.5}$–6L and $PM_{2.5}$–3H lungs. SOD1 expression was reduced in $PM_{2.5}$–3L lungs, while the reduction was diminished in $PM_{2.5}$–6L and $PM_{2.5}$–3H lungs. Compared to $PM_{2.5}$–3L lungs, $PM_{2.5}$–6L lungs exhibited higher levels of PRDX3 and similar levels of other antioxidant enzymes, while $PM_{2.5}$–3H lungs exhibited significantly higher levels of PRDX1 and SOD1, and lower levels of PRDX4. Considering that PRDX4 was the only identified antioxidant enzyme that was reduced by $PM_{2.5}$ exposure in a concentration-dependent manner, we postulated that PRDX4 reduction may play an important role in $PM_{2.5}$-induced pulmonary oxidative stress.

4. Discussion

Nowadays, air pollution or $PM_{2.5}$ has become a big threat to the respiratory and cardiovascular system [30–32]. Studies by others and ourselves have suggested that immune and inflammatory response, oxidative stress and DNA damage are potential mechanisms responsible for the adverse health effect of $PM_{2.5}$ [20,33–35]. In addition, transcriptomic analyses of $PM_{2.5}$-exposed 16HBE cells demonstrated that $PM_{2.5}$-induced DEGs were involved in inflammatory and immune response pathways, response to xenobiotic stimuli and metabolic response [16]. Another study revealed that $PM_{2.5}$ triggers infectious disease, cancers, cardiovascular diseases, and immune pathways in A549 cells [18]. It is therefore no strange that most of DEGs in $PM_{2.5}$–3L vs FA group were enriched in immune system and infectious disease pathways, such as Cytokine-cytokine receptor interaction, B cell receptor signaling pathway, *Staphylococcus aureus* infection, Antigen processing and presentation and Intestinal immune network for IgA production in the present study. Surprisingly, we found that the most significantly enriched KEGG pathway of DEGs in FA vs $PM_{2.5}$–3L or $PM_{2.5}$–6L groups is hematopoietic cell lineage. A revolutionary research study recently identified the lungs as a site of platelet biogenesis and a reservoir for hematopoietic progenitors [36]. Furthermore, previous studies have demonstrated that oxidative stress and inflammation are key regulators of hematopoietic stem cell fate in health and disease [37–39]. Thus, our findings indicate that the detrimental effect of $PM_{2.5}$

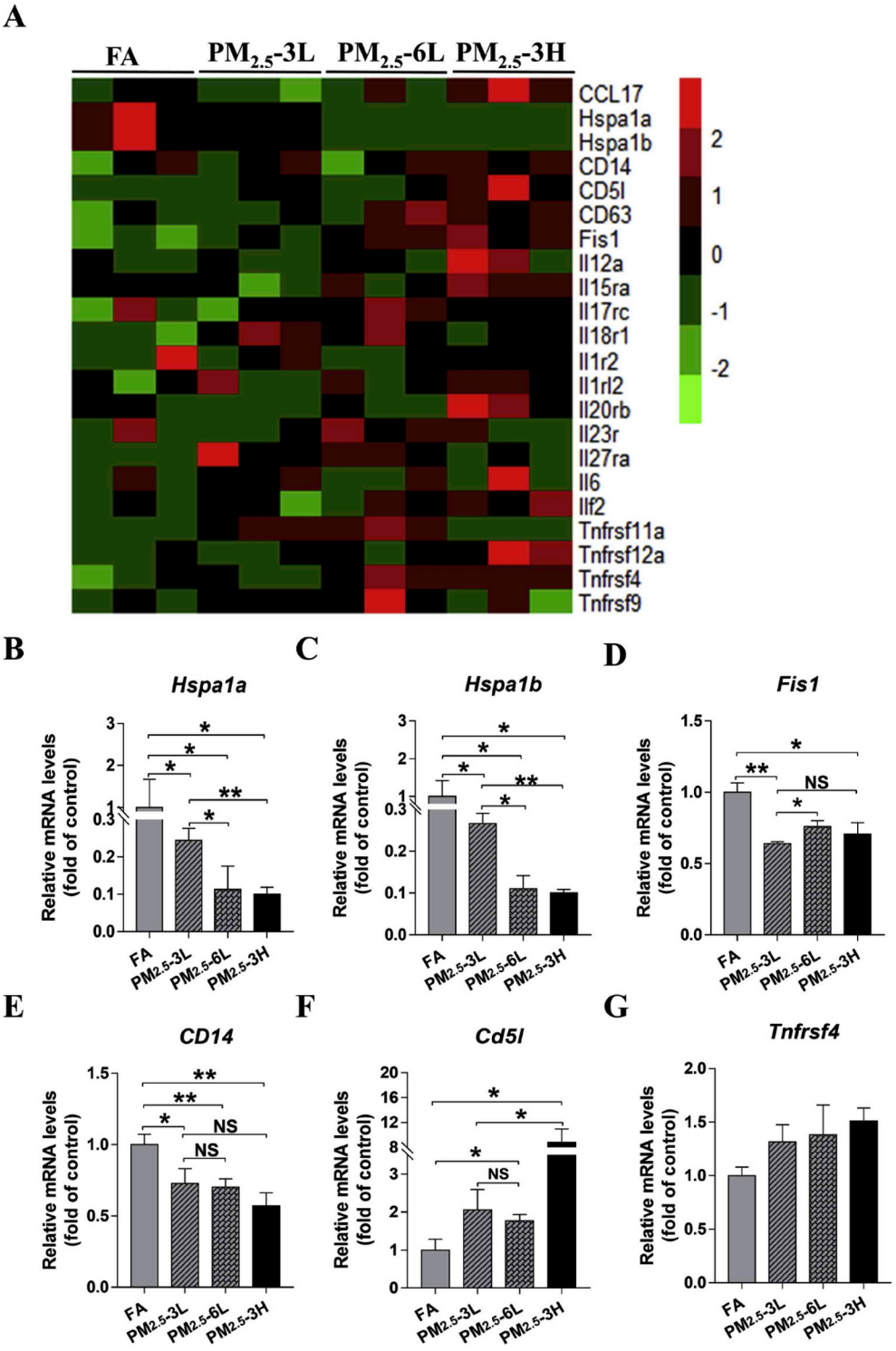

Fig. 5. Effect of $PM_{2.5}$ expose time and concentration on gene expression of inflammatory factors. (A) Heat map of gene expression of main inflammatory factors in FA-, $PM_{2.5}$-3L- and $PM_{2.5}$-3H-exposed lungs. To verify the RNA-seq results, mRNA levels of *Hspa1a* (B), *Hspa1b* (C), *Fis1* (D), *CD14* (E), *Cd5l*(F) and *Tnfrsf4* (G) were measured by real-time qPCR. N = 3, data are shown as mean ± SEM. *p < 0.05; **p < 0.01; NS, not significant.

exposure may include hematopoiesis dysregulation.

It is well documented that the cytotoxicity of $PM_{2.5}$ is dependent on its concentration. Epidemiological studies provide evidence that each 10 μg/m^3 elevation in $PM_{2.5}$ concentration was associated with significantly increased risk of all-cause mortality, COPD, asthma and cardiovascular disease [40]. *In vitro* experiments showed that $PM_{2.5}$ dose-dependently decreases cell viability in BEAS-2B [41], A549 [42], 16HBE [16] and macrophages [43]. In the present study, we also demonstrated that $PM_{2.5}$–3H exposure caused more severe lung injury and higher number of DEGs than did $PM_{2.5}$–3L. Interestingly, the top 2 most significantly enriched KEGG pathways of DEGs in FA vs $PM_{2.5}$–3H group were HCM and DCM, which are two common clinical subtypes of cardiomyopathy. Such pathway enrichment is in agreement with previous epidemiological studies, which confirmed that high $PM_{2.5}$ concentration is significantly associated with increased cardiovascular risk, including ischemic heart disease, heart failure, arrhythmias, and

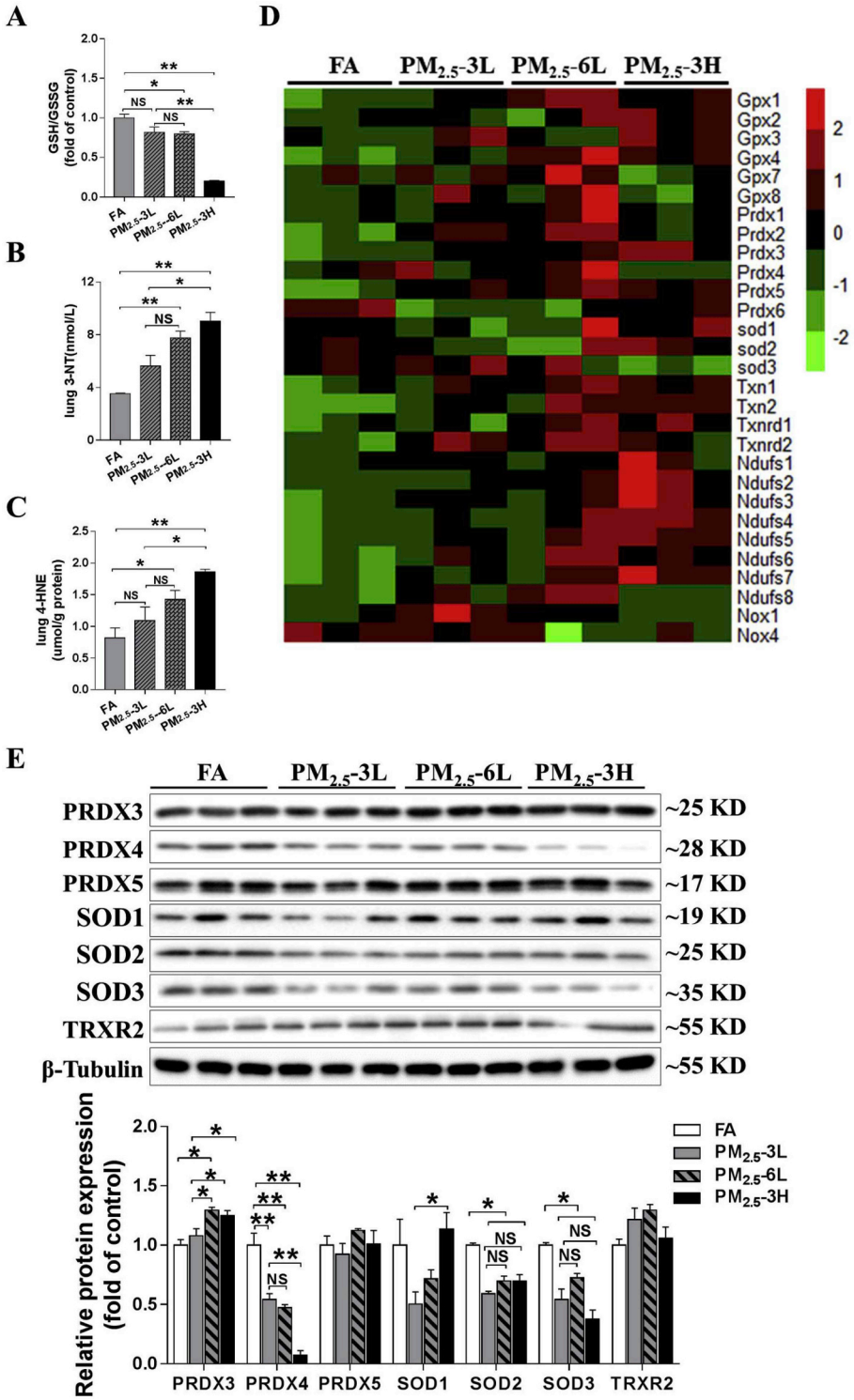

Fig. 6. $PM_{2.5}$ induced pulmonary oxidative stress in a concentration-dependent manner. After exposed to low or high concentration of $PM_{2.5}$ for 3–6 months, mice lungs were collected, and the GSH/GSSG ratio (A), 3′-NT (B) and 4-HNE (C) levels were measured. The expression of oxidative stress-related genes expression in FA-, $PM_{2.5}$-3L- and $PM_{2.5}$-3H-exposed lungs were listed as heat map (D). Lysates of lungs were examined by western blotting for the expression of peroxiredoxin 3 (PRDX3), PRDX4, PRDX5, superoxide dismutase 1 (SOD1), SOD2, SOD3 and thioredoxin reductase 2 (TRXR2). β-tubulin was used as a loading control (E). N = 3–5, data are shown as mean ± SEM; * indicates $p < 0.05$, ** indicates $p < 0.01$, NS, not significant.

cardiac death [44,45]. Using mouse model, we recently found that short-term $PM_{2.5}$ exposure is sufficient to induce a robust lung inflammation, vascular remodeling, and promote transition from left ventricular failure to right ventricular hypertrophy [34]. In addition, as the DEGs (*Mybpc1*, *Myh8/4/1*, *Myot*, and etc; Table S4) enriched in HCM and DCM pathways were mainly related to myopathy, we speculated that the activation of HCM and DCM pathways in $PM_{2.5}$-3H-exposed lungs might be associated with pulmonary vessel remodeling and muscularization. *Hspa1* encodes a 70 kDa heat shock protein, which exhibits a broad protective role in multiple diseases, including sepsis, insulin resistance and liver injury [46]. The anti-inflammatory mechanisms of *Hspa1* involves inhibition of NF-κB activation [47] and high-mobility group box 1 (HMGB1) release [48]. Furthermore, *Hspa1* facilitates DNA repair in Benzo[*a*]pyrene exposed 16HBE cells [49]. *Cd5l*, also called apoptosis inhibitor of macrophage (AIM), plays an important role in the control of immune homeostasis and inflammatory disease [50]. The finding shows that *Cd5l* is concentration-dependently upregulated in $PM_{2.5}$-exposed lung which is in agreement with previous study which demonstrated *Cd5l* was one of the significantly upregulated genes in welding fumes exposed rat lungs [51]. It has been

reported that deletion or blockade of *Cd5l* attenuates the inflammatory response in acute myocardial infarction [52] and experimental sepsis [53]. By contrast, overexpression of *Cd5l* in myeloid or alveolar type II epithelial cells induces systemic inflammation and adenocarcinoma in the lung [29,54]. Therefore, the significantly repressed *Hspa1* expression and dramatically up-regulated *Cd5l* may contribute to the enhanced pulmonary inflammation and fibrosis in $PM_{2.5}$-3H-exposed lungs.

Previous studies have demonstrated that $PM_{2.5}$ exposure could promote ROS production, which causes inflammatory cytokines release and DNA damage, and then leads to cell death and lung injury [1,11,55]. In the present study, we found that GSH/GSSG ratio and expression of some antioxidants enzymes (SOD2, SOD3 and PRDX4) were decreased, whereas 3′-NT and 4-HNE levels were increased in $PM_{2.5}$-exposed lungs. Consistent with our previous finding that $PM_{2.5}$ dose-dependently increases intracellular ROS in A549 cells [56], here we found that $PM_{2.5}$–3H caused greater pulmonary oxidative stress than did $PM_{2.5}$–3L. PRDX4 is an antioxidant enzyme located in the endoplasmic reticulum (ER) and plays an important role in H_2O_2 scavenging and protein folding in the ER [57]. PRDX4 deficiency has been found to exacerbate diethylnitrosamine-induced hepatic oxidative stress [58] and dextran sulfate sodium-induced intestinal inflammation [59]. Thus, the reduction of PRDX4 expression might be an important contributor for the elevated oxidative stress in $PM_{2.5}$-3H-exposed lungs.

In vitro experiments consistently demonstrated that $PM_{2.5}$ can affect cell viability, inflammation response and intracellular ROS in a time-dependent manner [55,60]. However, we found that there were no significant difference in system inflammation, lung injury, pulmonary GSH/GSSH ratio, 3′-NT and 4-HNE levels and antioxidant enzymes (PRDX4, PRDX5, SOD1, SOD2, SOD3 and TRXR2) expression between $PM_{2.5}$–3L and $PM_{2.5}$–6L groups, indicating that exposure time had no obvious effect on $PM_{2.5}$-induced inflammation and oxidative stress. This may due to the adaptive response triggered by $PM_{2.5}$ exposure. First, cytokines induced by early $PM_{2.5}$ exposure may contribute to mount an adaptive immune response to affect cytokines expression at late stage. For example, *Ccl17* expression was lower in $PM_{2.5}$–6L lungs than that of $PM_{2.5}$–3L lungs (Tables S2–S3). The finding that the DEGs were only significantly enriched in cytokine-cytokine receptor interaction pathways between $PM_{2.5}$–3L vs $PM_{2.5}$–6L, suggesting that the interaction among different cytokines may contribute to the similarity of lung injury. Second, $PM_{2.5}$ exposure could promote nuclear factor erythroid-2-related factor 2 (NRF2) nuclear translocation to orchestrate the antioxidant and detoxification genes [42,61]. The activation of NRF2 then protects cell against $PM_{2.5}$-induced cytotoxicity [42]. This kind of adaptive response may also explain why some antioxidant enzymes were upregulated in $PM_{2.5}$-exposed lungs, especially in lungs of $PM_{2.5}$–6L.

The present study has several limitations. It is well acknowledged that there are discrepancies between the mRNA and protein levels for some genes [62]. In this study, the profile of RNA-seq only provides a comprehensive overview of the entire transcriptome. However, the expression and activity levels of protein obtained from the study should be further examined. Moreover, additional analysis should be carried out to identify all the genes which have a trend for dose- or time-dependent changes in expression profile. These genes/pathways may be important for elucidating the harmful effect of $PM_{2.5}$ in respiratory system. Further studies are necessary in order to clarify the underlying mechanism whether the changes in gene expression profile are due to the direct or indirect/systematic effects of $PM_{2.5}$ on lung tissue.

In summary, our study indicated a strong concentration-response relationship between airborne $PM_{2.5}$ and lung injury. The effect of exposure time and concentration of airborne $PM_{2.5}$ on whole transcriptome profiling of mice lungs were illuminated by RNA-seq. As revealed by KEGG enrichment analysis, $PM_{2.5}$ mainly induced immune pathways, especially hematopoietic cell lineage pathway. Furthermore, our results suggest that *Hspa1*, *Cd5l* and *Prdx4* may play important roles in $PM_{2.5}$-induced pulmonary inflammation and oxidative stress. These data may provide deeper insight into the molecular mechanism for the harmful effect of $PM_{2.5}$.

Author disclosure statement

No competing financial interests exist.

Acknowledgments

This study was supported by grants from National Natural Science Foundation of China (91743104and 91643206) and University of Chinese Academy of Sciences. We would like to thank Fang Li, Shasha Zuo and Dandan Sun from University of Chinese Academy of Sciences for their kindly help in instrument operation.

Appendix A. Supplementary data

Supplementary data to this article can be found online at https://doi.org/10.1016/j.redox.2019.101264.

References

[1] N. Li, M. Hao, R.F. Phalen, W.C. Hinds, A.E. Nel, Particulate air pollutants and asthma. A paradigm for the role of oxidative stress in PM-induced adverse health effects, Clin. Immunol. 109 (3) (2003) 250–265.
[2] I. Hertz-Picciotto, R.J. Baker, P.S. Yap, M. Dostal, J.P. Joad, M. Lipsett, T. Greenfield, C.E. Herr, I. Benes, R.H. Shumway, K.E. Pinkerton, R. Sram, Early childhood lower respiratory illness and air pollution, Environ. Health Perspect. 115 (10) (2007) 1510–1518.
[3] T. Sint, J.F. Donohue, A.J. Ghio, Ambient air pollution particles and the acute exacerbation of chronic obstructive pulmonary disease, Inhal. Toxicol. 20 (1) (2008) 25–29.
[4] G.B. Hamra, N. Guha, A. Cohen, F. Laden, O. Raaschou-Nielsen, J.M. Samet, P. Vineis, F. Forastiere, P. Saldiva, T. Yorifuji, D. Loomis, Outdoor particulate matter exposure and lung cancer: a systematic review and meta-analysis, Environ. Health Perspect. 122 (9) (2014) 906–911.
[5] V.C. Pun, F. Kazemiparkouhi, J. Manjourides, H.H. Suh, Long-term PM2.5 exposure and respiratory, cancer, and cardiovascular mortality in older US adults, Am. J. Epidemiol. 186 (8) (2017) 961–969.
[6] M.J. Daniels, F. Dominici, J.M. Samet, S.L. Zeger, Estimating particulate matter-mortality dose-response curves and threshold levels: an analysis of daily time-series for the 20 largest US cities, Am. J. Epidemiol. 152 (5) (2000) 397–406.
[7] C. Chen, C. Li, Y. Li, J. Liu, C. Meng, J. Han, Y. Zhang, D. Xu, Short-term effects of ambient air pollution exposure on lung function: a longitudinal study among healthy primary school children in China, Sci. Total Environ. 645 (2018) 1014–1020.
[8] F. Dominici, R.D. Peng, M.L. Bell, L. Pham, A. McDermott, S.L. Zeger, J.M. Samet, Fine particulate air pollution and hospital admission for cardiovascular and respiratory diseases, JAMA 295 (10) (2006) 1127–1134.
[9] A. Zanobetti, M. Franklin, P. Koutrakis, J. Schwartz, Fine particulate air pollution and its components in association with cause-specific emergency admissions, Environ. Health : A Glob. Access Sci. Source 8 (2009) 58.
[10] S. Jiang, J. Zhou, J. Zhang, X. Du, X. Zeng, K. Pan, Y. Xie, H. Kan, Q. Sun, J. Cai, J. Zhao, The severity of lung injury and metabolic disorders induced by ambient PM2.5 exposure is associated with cumulative dose, Inhal. Toxicol. (2018) 1–8.
[11] D.R. Riva, C.B. Magalhaes, A.A. Lopes, T. Lancas, T. Mauad, O. Malm, S.S. Valenca, P.H. Saldiva, D.S. Faffe, W.A. Zin, Low dose of fine particulate matter (PM2.5) can induce acute oxidative stress, inflammation and pulmonary impairment in healthy mice, Inhal. Toxicol. 23 (5) (2011) 257–267.
[12] C. Zhao, J.P. Liao, W.L. Chu, S.X. Wang, T.S. Yang, Y.H. Tao, G.F. Wang, Involvement of TLR2 and TLR4 and Th1/Th2 shift in inflammatory responses induced by fine ambient particulate matter in mice, Inhal. Toxicol. 24 (13) (2012) 918–927.
[13] U. Vattanasit, P. Navasumrit, M.B. Khadka, J. Kanitwithayanun, J. Promvijit, H. Autrup, M. Ruchirawat, Oxidative DNA damage and inflammatory responses in cultured human cells and in humans exposed to traffic-related particles, Int. J. Hyg Environ. Health 217 (1) (2014) 23–33.
[14] S.M. Oh, H.R. Kim, Y.J. Park, S.Y. Lee, K.H. Chung, Organic extracts of urban air pollution particulate matter (PM2.5)-induced genotoxicity and oxidative stress in human lung bronchial epithelial cells (BEAS-2B cells), Mutat. Res. Genet. Toxicol. Environ. Mutagen 723 (2) (2011) 142–151.
[15] B.F. Cachon, S. Firmin, A. Verdin, L. Ayi-Fanou, S. Billet, F. Cazier, P.J. Martin, F. Aissi, D. Courcot, A. Sanni, P. Shirali, Proinflammatory effects and oxidative stress within human bronchial epithelial cells exposed to atmospheric particulate matter (PM2.5 and PM > 2.5) collected from Cotonou, Benin, Environ. Pollut. 185 (2014) 340–351.
[16] Z. Zhou, Y. Liu, F. Duan, M. Qin, F. Wu, W. Sheng, L. Yang, J. Liu, K. He, Transcriptomic analyses of the biological effects of airborne PM2.5 exposure on

human bronchial epithelial cells, PLoS One 10 (9) (2015) e0138267.
[17] L. Zheng, S. Liu, G. Zhuang, J. Xu, Q. Liu, X. Zhang, C. Deng, Z. Guo, W. Zhao, T. Liu, Y. Wang, Y. Zhang, J. Lin, Q. Wang, G. Sui, Signal transductions of BEAS-2B cells in response to carcinogenic PM2.5 exposure based on a microfluidic system, Anal. Chem. 89 (10) (2017) 5413–5421.
[18] X. Lei, J.E. Muscat, Z. Huang, C. Chen, G. Xiu, J. Chen, Differential transcriptional changes in human alveolar epithelial A549 cells exposed to airborne PM2.5 collected from Shanghai, China, Environ. Sci. Pollut. Res. Int. 25 (33) (2018) 33656–33666.
[19] B. Yang, X.M. Li, D.M. Chen, C.L. Xiao, Effects of fine air particulates on gene expression in non-small-cell lung cancer, Adv. Med. Sci. 62 (2) (2017) 295–301.
[20] H. Wang, X. Shen, G. Tian, X. Shi, W. Huang, Y. Wu, L. Sun, C. Peng, S. Liu, Y. Huang, X. Chen, F. Zhang, Y. Chen, W. Ding, Z. Lu, AMPKalpha2 deficiency exacerbates long-term PM2.5 exposure-induced lung injury and cardiac dysfunction, Free Radical Biol. Med. 121 (2018) 202–214.
[21] A.M. Bolger, M. Lohse, B. Usadel, Trimmomatic: a flexible trimmer for Illumina sequence data, Bioinformatics 30 (15) (2014) 2114–2120.
[22] D. Kim, B. Langmead, S.L. Salzberg, HISAT: a fast spliced aligner with low memory requirements, Nat. Methods 12 (4) (2015) 357–360.
[23] B. Langmead, S.L. Salzberg, Fast gapped-read alignment with Bowtie 2, Nat. Methods 9 (4) (2012) 357–359.
[24] B. Li, C.N. Dewey, RSEM: accurate transcript quantification from RNA-Seq data with or without a reference genome, BMC Bioinf. 12 (2011) 323.
[25] L. Wang, Z. Feng, X. Wang, X. Wang, X. Zhang, DEGseq: an R package for identifying differentially expressed genes from RNA-seq data, Bioinformatics 26 (1) (2010) 136–138.
[26] Q. Shen, H. Zhang, Y. Su, Z. Wen, Z. Zhu, G. Chen, L. Peng, C. Du, H. Xie, H. Li, X. Lv, C. Lu, Y. Xia, W. Tang, Identification of two novel PCDHA9 mutations associated with Hirschsprung's disease, Gene 658 (2018) 96–104.
[27] W. Van Molle, B. Wielockx, T. Mahieu, M. Takada, T. Taniguchi, K. Sekikawa, C. Libert, HSP70 protects against TNF-induced lethal inflammatory shock, Immunity 16 (5) (2002) 685–695.
[28] H. Nishimura, M. Emoto, K. Kimura, Y. Yoshikai, Hsp70 protects macrophages infected with Salmonella choleraesuis against TNF-alpha-induced cell death, Cell Stress Chaperones 2 (1) (1997) 50–59.
[29] Y. Li, P. Qu, L. Wu, B. Li, H. Du, C. Yan, Api6/AIM/Spalpha/CD5L overexpression in alveolar type II epithelial cells induces spontaneous lung adenocarcinoma, Cancer Res. 71 (16) (2011) 5488–5499.
[30] Y.F. Xing, Y.H. Xu, M.H. Shi, Y.X. Lian, The impact of PM2.5 on the human respiratory system, J. Thorac. Dis. 8 (1) (2016) E69–E74.
[31] J. Zhao, L. Bo, C. Gong, P. Cheng, H. Kan, Y. Xie, W. Song, Preliminary study to explore gene-PM2.5 interactive effects on respiratory system in traffic policemen, Int. J. Occup. Med. Environ. Health 28 (6) (2015) 971–983.
[32] T. Xu, J. Hou, J. Cheng, R. Zhang, W. Yin, C. Huang, X. Zhu, W. Chen, J. Yuan, Estimated individual inhaled dose of fine particles and indicators of lung function: a pilot study among Chinese young adults, Environ. Pollut. 235 (2018) 505–513.
[33] S. Liu, W. Zhang, F. Zhang, P. Roepstorff, F. Yang, Z. Lu, W. Ding, TMT-based quantitative proteomics analysis reveals airborne PM2.5-induced pulmonary fibrosis, Int. J. Environ. Res. Public Health 16 (1) (2018).
[34] W. Yue, L. Tong, X. Liu, X. Weng, X. Chen, D. Wang, S.C. Dudley, E.K. Weir, W. Ding, Z. Lu, Y. Xu, Y. Chen, Short term Pm2.5 exposure caused a robust lung inflammation, vascular remodeling, and exacerbated transition from left ventricular failure to right ventricular hypertrophy, Redox Biol. 22 (2019) 101161.
[35] A.A.F. de Oliveira, T.F. de Oliveira, M.F. Dias, M.H.G. Medeiros, P. Di Mascio, M. Veras, M. Lemos, T. Marcourakis, P.H.N. Saldiva, A.P.M. Loureiro, Genotoxic and epigenotoxic effects in mice exposed to concentrated ambient fine particulate matter (PM2.5) from Sao Paulo city, Brazil, Part. Fibre Toxicol. 15 (1) (2018) 40.
[36] E. Lefrancais, G. Ortiz-Munoz, A. Caudrillier, B. Mallavia, F.C. Liu, D.M. Sayah, E.E. Thornton, M.B. Headley, T. David, S.R. Coughlin, M.F. Krummel, A.D. Leavitt, E. Passegue, M.R. Looney, The lung is a site of platelet biogenesis and a reservoir for haematopoietic progenitors, Nature 544 (7648) (2017) 105–+.
[37] E.M. Pietras, Inflammation: a key regulator of hematopoietic stem cell fate in health and disease, Blood 130 (15) (2017) 1693–1698.
[38] D.Q. Tan, T. Suda, Reactive oxygen species and mitochondrial homeostasis as regulators of stem cell fate and function, Antioxidants Redox Signal. 29 (2) (2018) 149–168.
[39] H. Jung, I. Choi, Thioredoxin-interacting protein, hematopoietic stem cells, and hematopoiesis, Curr. Opin. Hematol. 21 (4) (2014) 265–270.
[40] C.A. Pope 3rd, R.T. Burnett, M.J. Thun, E.E. Calle, D. Krewski, K. Ito, G.D. Thurston, Lung cancer, cardiopulmonary mortality, and long-term exposure to fine particulate air pollution, JAMA 287 (9) (2002) 1132–1141.
[41] Y. Li, J. Duan, M. Yang, Y. Li, L. Jing, Y. Yu, J. Wang, Z. Sun, Transcriptomic analyses of human bronchial epithelial cells BEAS-2B exposed to atmospheric fine particulate matter PM2.5, Toxicol. Vitro : Int. J. Publ. Assoc. BIBRA 42 (2017) 171–181.
[42] H. Wang, Y. Guo, L. Liu, L. Guan, T. Wang, L. Zhang, Y. Wang, J. Cao, W. Ding, F. Zhang, Z. Lu, DDAH1 plays dual roles in PM2.5 induced cell death in A549 cells, Biochim. Biophys. Acta 1860 (12) (2016) 2793–2801.
[43] Y. Zhang, S. Wang, J. Zhu, C. Li, T. Zhang, H. Liu, Q. Xu, X. Ye, L. Zhou, L. Ye, Effect of atmospheric PM2.5 on expression levels of NF-kappaB genes and inflammatory cytokines regulated by NF-kappaB in human macrophage, Inflammation 41 (3) (2018) 784–794.
[44] W. Xie, G. Li, D. Zhao, X. Xie, Z. Wei, W. Wang, M. Wang, G. Li, W. Liu, J. Sun, Z. Jia, Q. Zhang, J. Liu, Relationship between fine particulate air pollution and ischaemic heart disease morbidity and mortality, Heart 101 (4) (2015) 257–263.
[45] C.A. Pope 3rd, M.C. Turner, R.T. Burnett, M. Jerrett, S.M. Gapstur, W.R. Diver, D. Krewski, R.D. Brook, Relationships between fine particulate air pollution, cardiometabolic disorders, and cardiovascular mortality, Circ. Res. 116 (1) (2015) 108–115.
[46] K. Levada, N. Guldiken, X. Zhang, G. Vella, F.R. Mo, L.P. James, J. Haybaeck, S.M. Kessler, A.K. Kiemer, T. Ott, D. Hartmann, N. Huser, M. Ziol, C. Trautwein, P. Strnad, Hsp72 protects against liver injury via attenuation of hepatocellular death, oxidative stress, and JNK signaling, J. Hepatol. 68 (5) (2018) 996–1005.
[47] P.W. Sheppard, X. Sun, M. Khammash, R.G. Giffard, Overexpression of heat shock protein 72 attenuates NF-kappaB activation using a combination of regulatory mechanisms in microglia, PLoS Comput. Biol. 10 (2) (2014) e1003471.
[48] D. Tang, R. Kang, W. Xiao, H. Wang, S.K. Calderwood, X. Xiao, The anti-inflammatory effects of heat shock protein 72 involve inhibition of high-mobility-group box 1 release and proinflammatory function in macrophages, J. Immunol. 179 (2) (2007) 1236–1244.
[49] Y.Y. Duan, S.L. Huang, J. Yang, P.Y. Niu, Z.Y. Gong, X.Y. Liu, L.L. Xin, R.W. Currie, T.C. Wu, HspA1A facilitates DNA repair in human bronchial epithelial cells exposed to Benzo[a]pyrene and interacts with casein kinase 2, Cell Stress Chaperones 19 (2) (2014) 271–279.
[50] L. Sanjurjo, G. Aran, N. Roher, A.F. Valledor, M.R. Sarrias, AIM/CD5L: a key protein in the control of immune homeostasis and inflammatory disease, J. Leukoc. Biol. 98 (2) (2015) 173–184.
[51] J.H. Oh, M.J. Yang, J.D. Heo, Y.S. Yang, H.J. Park, S.M. Park, M.S. Kwon, C.W. Song, S. Yoon, I.J. Yu, Inflammatory response in rat lungs with recurrent exposure to welding fumes: a transcriptomic approach, Toxicol. Ind. Health 28 (3) (2012) 203–215.
[52] T. Nishikido, J. Oyama, A. Shiraki, H. Komoda, K. Node, Deletion of apoptosis inhibitor of macrophage (AIM)/CD5L attenuates the inflammatory response and infarct size in acute myocardial infarction, J. Am. Heart Assoc. 5 (4) (2016) e002863.
[53] X. Gao, X. Yan, Y. Yin, X. Lin, Q. Zhang, Y. Xia, J. Cao, Therapeutic targeting of apoptosis inhibitor of macrophage/CD5L in sepsis, Am. J. Respir. Cell Mol. Biol. 60 (3) (2019) 323–334.
[54] P. Qu, H. Du, Y. Li, C. Yan, Myeloid-specific expression of Api6/AIM/Sp alpha induces systemic inflammation and adenocarcinoma in the lung, J. Immunol. 182 (3) (2009) 1648–1659.
[55] X. Deng, F. Zhang, W. Rui, F. Long, L. Wang, Z. Feng, D. Chen, W. Ding, PM2.5-induced oxidative stress triggers autophagy in human lung epithelial A549 cells, Toxicol. Vitro : Int. J. Publ. Assoc. BIBRA 27 (6) (2013) 1762–1770.
[56] X. Deng, F. Zhang, L. Wang, W. Rui, F. Long, Y. Zhao, D. Chen, W. Ding, Airborne fine particulate matter induces multiple cell death pathways in human lung epithelial cells, Apoptosis : Int. J. Program. Cell Death 19 (7) (2014) 1099–1112.
[57] E. Zito, PRDX4, an endoplasmic reticulum-localized peroxiredoxin at the crossroads between enzymatic oxidative protein folding and nonenzymatic protein oxidation, Antioxidants Redox Signal. 18 (13) (2013) 1666–1674.
[58] X. Guo, H. Noguchi, N. Ishii, T. Homma, T. Hamada, T. Hiraki, J. Zhang, K. Matsuo, S. Yokoyama, H. Ishibashi, T. Fukushige, T. Kanekura, J. Fujii, H. Uramoto, A. Tanimoto, S. Yamada, The association of peroxiredoxin 4 with the initiation and progression of hepatocellular carcinoma, Antioxidants Redox Signal. 30 (10) (2019) 1271–1284.
[59] T. Takagi, T. Homma, J. Fujii, N. Shirasawa, H. Yoriki, Y. Hotta, Y. Higashimura, K. Mizushima, Y. Hirai, K. Katada, K. Uchiyama, Y. Naito, Y. Itoh, Elevated ER stress exacerbates dextran sulfate sodium-induced colitis in PRDX4-knockout mice, Free Radical Biol. Med. 134 (2018) 153–164.
[60] I. Abbas, G. Badran, A. Verdin, F. Ledoux, M. Roumie, J.M. Lo Guidice, D. Courcot, G. Garcon, In vitro evaluation of organic extractable matter from ambient PM2.5 using human bronchial epithelial BEAS-2B cells: cytotoxicity, oxidative stress, pro-inflammatory response, genotoxicity, and cell cycle deregulation, Environ. Res. 171 (2019) 510–522.
[61] X. Deng, W. Rui, F. Zhang, W. Ding, PM2.5 induces Nrf2-mediated defense mechanisms against oxidative stress by activating PIK3/AKT signaling pathway in human lung alveolar epithelial A549 cells, Cell Biol. Toxicol. 29 (3) (2013) 143–157.
[62] D. Wang, Discrepancy between mRNA and protein abundance: insight from information retrieval process in computers, Comput. Biol. Chem. 32 (6) (2008) 462–468.